Hope Creek Generating Station
Facility Operating License NPF-57
Docket No. 50-354

Extended Power Uprate

Hydrodynamic Loads on Hope Creek Unit 1 Steam Dryer to 200 Hz
CDI Report 06-17, Revision 3
April 2007

C.D.I. Report No. 06-17

Hydrodynamic Loads on Hope Creek Unit 1 Steam Dryer to 200 Hz

Revision 3

Prepared by

Continuum Dynamics, Inc.
34 Lexington Avenue
Ewing, NJ 08618

Prepared under Purchase Order No. 4500341046 for

Nuclear Business Unit, PSEG Nuclear LLC
Materials Center, Alloway Creek Neck Road
Hancocks Bridge, NJ 08038

Approved by

Alan J. Bilanin

Reviewed by

Milton E. Teske

April 2007

Executive Summary

Measured in-plant pressure time-history data in the four main steam lines of Hope Creek Unit 1 (HC1), at the eight strain gage locations at Current Licensed Thermal Power (CLTP), are processed by a dynamic model of the steam delivery system to predict loads on the steam dryer. These measured data are used with a validated acoustic circuit model to predict the fluctuating pressures anticipated across components of the steam dryer in the reactor vessel. The hydrodynamic load data may then be used by a structural analyst to assess the structural adequacy of the steam dryer in HC1.

Additional measured one-eighth scale pressure time-history data, at CLTP and Extended Power Uprate (EPU), are converted to full-scale pressure time-history data and used to predict hydrodynamic loads on the steam dryer as well. EPU for HC1 is 115% CLTP.

This effort provides PSEG with a dryer dynamic load definition that comes directly from measured in-plant data and subscale test data, and the application of a validated acoustic circuit model, at power levels where the pressure data were acquired.

Summary of Changes from Revision 2 to Revision 3

Revision 3 of C.D.I. Report No. 06-17 reflects changes due to information developed after release of Revision 2, as explained below.

Updates for CLTP in-plant data:

Revision 2 of C.D.I. Report No. 06-17 was based on the May 2006 in-plant main steam line strain gage data. The reported results were derived using strain gage measurements from main steam lines A and B only, since the lower strain gage channels on main steam lines C and D failed during plant startup. This loss of data required Hope Creek Generating Station (HCGS) to bound the in-plant loads by developing an algorithm that assumed that the missing C and D strain gage data were mirror images of the available B and A data, respectively, but with an adjustment of the phasing of the C and D data to maximize the predicted load on the dryer.

In February 2007, during a maintenance outage, HCGS restored the failed strain gages on main steam lines C and D. Subsequently, HCGS successfully collected in-plant data from all four main steam lines at 100% CLTP conditions. Reference [1] provides the updated in-plant information and comparison of the two loads, and demonstrates that the 2006 loads were conservative with respect to the more accurate 2007 load calculation. Since there is now no need to rely on the previously developed algorithm, all discussions related to this algorithm are removed from C.D.I. Report No. 06-17.

In addition, the following tables and figures from Revision 2 are deleted in Revision 3:

- Tables 3.1 and 3.3: This information is now available as Tables 3.1 and 3.3 of [1].
- Table 3.2: This table provided information on the number and locations of the SRVs in the HCGS main steam lines, to show the similarity between main steam lines A and D and main steam lines B and C, respectively, and support the algorithm that is no longer needed.
- Tables 3.4 and 3.5: Susquehanna data to support the algorithm are no longer needed.
- Figures 3.1 and 3.2: The PSDs of the in-plant strain gage data at CLTP conditions for main steam lines A and B, respectively, are now provided in Figure 3.1 of [1] for all four main steam lines.
- Figure 3.3: Coherence of strain gage data at CLTP conditions for main steam lines A and B is now provided for all main steam lines in Figure 3.2 of [1].
- Figures 3.4 and 3.5: Susquehanna data to support the algorithm are no longer needed.
- Figure 4.5: The results of the nodal analysis for the in-plant data at CLTP conditions are now provided in Figure 4.1 of [1].

- Figure 4.6: The PSDs at nodes 7 and 99, based on in-plant data at CLTP conditions, are now provided in Figure 4.3 of [1].

- Figure 4.7: Susquehanna data to support the algorithm are no longer needed.

Changes in the Scale Model Test (SMT) results

Following completion of the SMT tests in 2006, it was recognized that the SMT results were excessively conservative, as documented in Revision 2 of C.D.I. Report No. 06-17. A key reason for this conservatism was that the initial SMT results predicted the onset of SRV acoustic resonance at approximately halfway between 80% and 90% CLTP conditions, whereas in-plant data showed that there was no SRV acoustic resonance at or below 100% CLTP conditions. HCGS subsequently requested C.D.I. to re-benchmark the SMT to provide more accurate loads. After re-benchmarking, the SMT predicted the onset of SRV acoustic resonance at CLTP conditions, which are still conservative but not as over-conservative as before.

C.D.I. Report No. 06-17 is updated in Revision 3 to provide the revised CLTP and EPU SMT summary data. The following figures and tables were revised:

- Figures 3.6 to 3.13 and Figures 4.8 to 4.10: The changes now reflect the revised SMT CLTP and EPU data. These figures have been renumbered to Figures 3.1 to 3.8 and to Figures 4.5 to 4.7, respectively.

- Table 3.6: The revised table provides the pressure levels in the main steam lines at CLTP and EPU conditions to now reflect the revised CLTP and EPU conditions. This table has been renumbered as Table 3.1.

Table of Contents

1. Introduction

In Spring 2005 Exelon installed new steam dryers into Quad Cities Unit 2 (QC2) and Quad Cities Unit 1. This replacement design, developed by General Electric, sought to improve dryer performance and overcome structural inadequacies identified on the original dryers, which had been in place for the last 30 years. As a means for confirming the adequacy of the steam dryer, the QC2 dryer was instrumented with pressure sensors at 27 locations. These pressures formed the set of data used to validate the predictions of an acoustic circuit model under development by Continuum Dynamics, Inc. for several years [2]. The results of this benchmark exercise [3] confirmed the predictive ability of the acoustic circuit model for pressure loading across the dryer. This model, validated against the Exelon full scale data, is used in this effort.

This report applies this validated acoustic circuit model to the Hope Creek Unit 1 (HC1) steam dryer and main steam line geometry. Data obtained from the four main steam lines are used to generate predictions of the pressure loading on the HC1 dryer at Current Licensed Thermal Power (CLTP). In addition, data obtained from a one-eighth scale model of the HC1 steam delivery system are used to generate full-scale predictions of the pressure loading on the HC1 dryer at CLTP and at Extended Power Uprate (EPU) conditions.

2. Modeling Considerations

The HC1 steam supply system is broken into two distinct analyses: a Helmholtz solution within the steam dome and an acoustic circuit analysis in the main steam lines. This section of the report highlights the two approaches taken here.

2.1 Helmholtz Analysis

A cross-section of the steam dome (and steam dryer) is shown below in Figure 2.1, with HC1 dimensions as shown. The complex three-dimensional geometry is rendered onto a uniformly-spaced rectangular grid (with mesh spacing of approximately 1.5 inches), and a solution is obtained for the Helmholtz equation

$$\frac{\partial^2 P}{\partial x^2}+\frac{\partial^2 P}{\partial y^2}+\frac{\partial^2 P}{\partial z^2}+\frac{\omega^2}{a^2}P=\nabla^2 P+\frac{\omega^2}{a^2}P=0$$

where P is the pressure at a grid point, ω is frequency, and a is acoustic speed in steam.

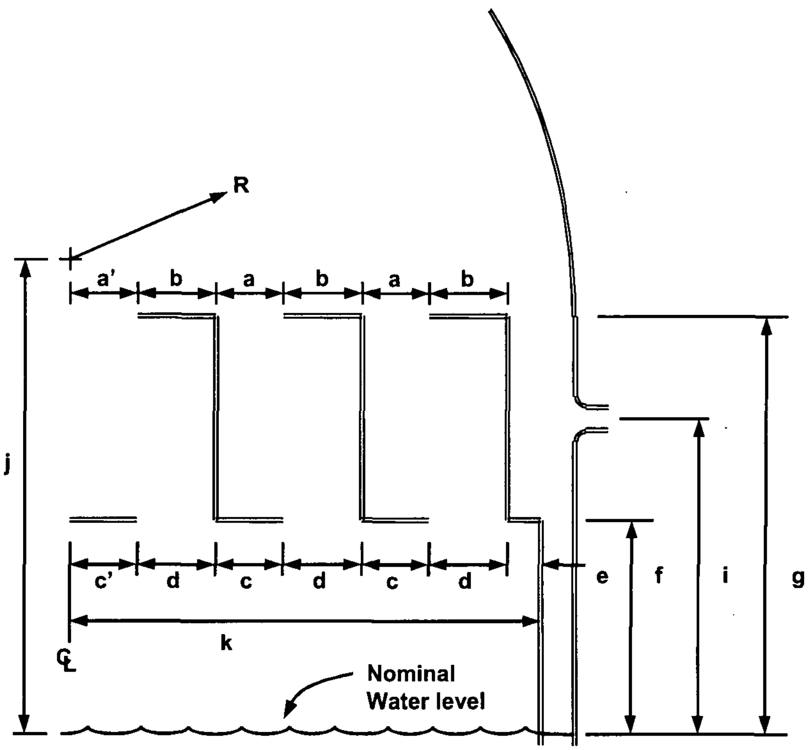

Figure 2.1. Cross-sectional description of the steam dome and dryer, with the verified HC1 dimensions of a' = 15.0, a = 17.5 in, b = 13.5 in, c' = 21.0 in, c = 15.0 in, d = 16.0 in, e = 21.0 in, f = 73.0 in, g = 163.0 in, i = 96.5 in, j = 183.0 in, k = 120.0 in, and R = 125.5 in.

This equation is solved for incremental frequencies from 0 to 200 Hz, subject to the boundary conditions

$$\frac{dP}{dn} = 0$$

normal to all solid surfaces (the steam dome wall and interior and exterior surfaces of the dryer),

$$\frac{dP}{dn} \propto \frac{i\omega}{a} P$$

normal to the nominal water level surface, and unit pressure applied to one inlet to a main steam line and zero applied to the other three.

2.2 Acoustic Circuit Analysis

The Helmholtz solution within the steam dome is coupled to an acoustic circuit solution in the main steam lines. Pulsations in a single-phase compressible medium, where acoustic wavelengths are long compared to component dimensions, and in particular long compared to transverse dimensions (directions perpendicular to the primary flow directions), lend themselves to application of the acoustic circuit methodology. If the analysis is restricted to frequencies below 200 Hz, acoustic wavelengths are approximately 8 feet in length and wavelengths are therefore long compared to most components of interest, such as branch junctions.

Acoustic circuit analysis divides the main steam lines into elements which are each characterized, as sketched in Figure 2.2, by a length L, a cross-sectional area A, a fluid mean density $\bar{\rho}$, a fluid mean flow velocity $\bar{U}$, and a fluid mean acoustic speed $\bar{a}$.

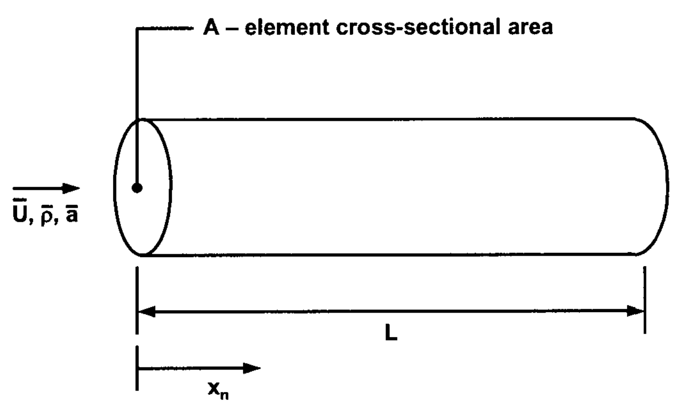

Figure 2.2. Schematic of an element in the acoustic circuit analysis, with length L and cross-sectional area A.

Application of acoustic circuit methodology generates solutions for the fluctuating pressure P_n and velocity u_n in the n^{th} element of the form

$$P_n = \left[A_n e^{ik_{1n}X_n} + B_n e^{ik_{2n}X_n}\right] e^{i\omega t}$$

$$u_n = -\frac{1}{\rho \bar{a}^2}\left[\frac{\left(\omega + \bar{U}_n k_{1n}\right)}{k_{1n}} A_n e^{ik_{1n}X_n} + \frac{\left(\omega + \bar{U}_n k_{2n}\right)}{k_{2n}} B_n e^{ik_{2n}X_n}\right] e^{i\omega t}$$

where harmonic time dependence of the form $e^{i\omega t}$ has been assumed. The wave numbers k_{1n} and k_{2n} are the two complex roots of the equation

$$k_n^{\ 2} + i\frac{f_n\left|\bar{U}_n\right|}{D_n \bar{a}^2}\left(\omega + \bar{U}_n k_n\right) - \frac{1}{\bar{a}^2}\left(\omega + \bar{U}_n k_n\right)^2 = 0$$

where f_n is the pipe friction factor for element n, D_n is the hydrodynamic diameter for element n, and $i = \sqrt{-1}$. A_n and B_n are complex constants which are a function of frequency and are determined by satisfying continuity of pressure and mass conservation at element junctions.

The main steam line piping geometry is summarized in Table 2.1.

Table 2.1. Main steam line lengths at HC1. The main steam lines are 26 inch Schedule 80 (ID = 23.647 in) to the strain gages.

Main Steam Line	Distance to First Strain Gage (ft)	Distance to Second Strain Gage (ft)
A	9.71	45.83
B	9.71	45.71
C	9.71	45.71
D	9.71	45.83

3. Input Pressure Data

3.1 In-Plant CLTP

The information originally provided in Section 3.1 of Revision 2 of this report included the May 2006 in-plant data for main steam lines A and B. This information is now superseded by Section 3.1 of [1], providing the February 2007 in-plant data for all four main steam lines.

3.2 In-Plant Conservatism

The information originally provided in Section 3.2 of Revision 2 of this report was used to support an algorithm developed to estimate dryer loads from in-plant data on only two main steam lines. Section 3.2 also used information from Susquehanna. Since the need for the algorithm has been eliminated by obtaining in-plant data on all four main steam lines, the information in Revision 2 is no longer required. Note that Section 4, Figure 4.1, and Figure 4.3 of [1] demonstrate that the in-plant data taken in May 2006, which relied on only two main steam lines and an algorithm for conservatively bounding the load, provided conservative steam dryer loadings when compared with the in-plant data taken in February 2007.

3.3 Subscale CLTP and EPU Data

A test was conducted in 2006 on a one-eighth scale representation of the HC1 steam delivery system. This work, detailed in [4], predicted the CLTP and EPU loads to be anticipated on the HC1 steam dryer. These subscale loads were corrected back to full scale by correcting the frequency of data collection (reducing the frequency by a factor of 5.7) and the pressure magnitude (multiplying the pressure by a factor of 5.2) on the eight pressure transducers on the four main steam lines.

Subsequent to the 2006 SMT effort, a re-benchmarking of the one-eighth scale facility was performed in January 2007. Figures 3.1 to 3.8, which are the PSDs of the eight SMT pressure transducers, and Table 3.1, which provides the pressure level summary, were revised to reflect the results of the SMT re-benchmarking. Note that a PSD comparison of the SMT data at CLTP conditions, against the in-plant CLTP data for these eight locations, is provided in Figure 3.4 of [1].

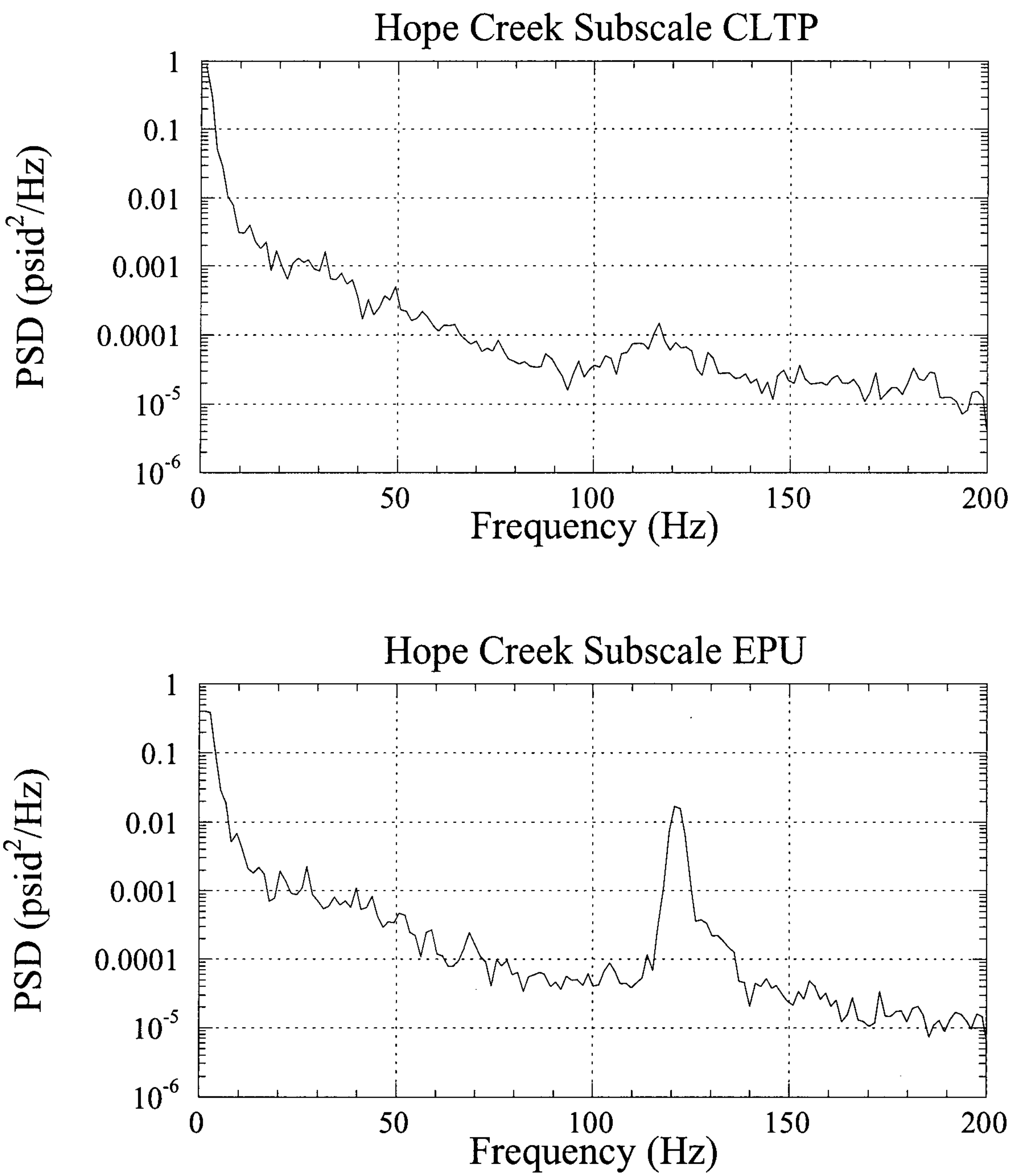

Figure 3.1. PSD comparison of pressure transducer data at CLTP (top) and EPU (bottom) conditions, for main steam line A, upstream location.

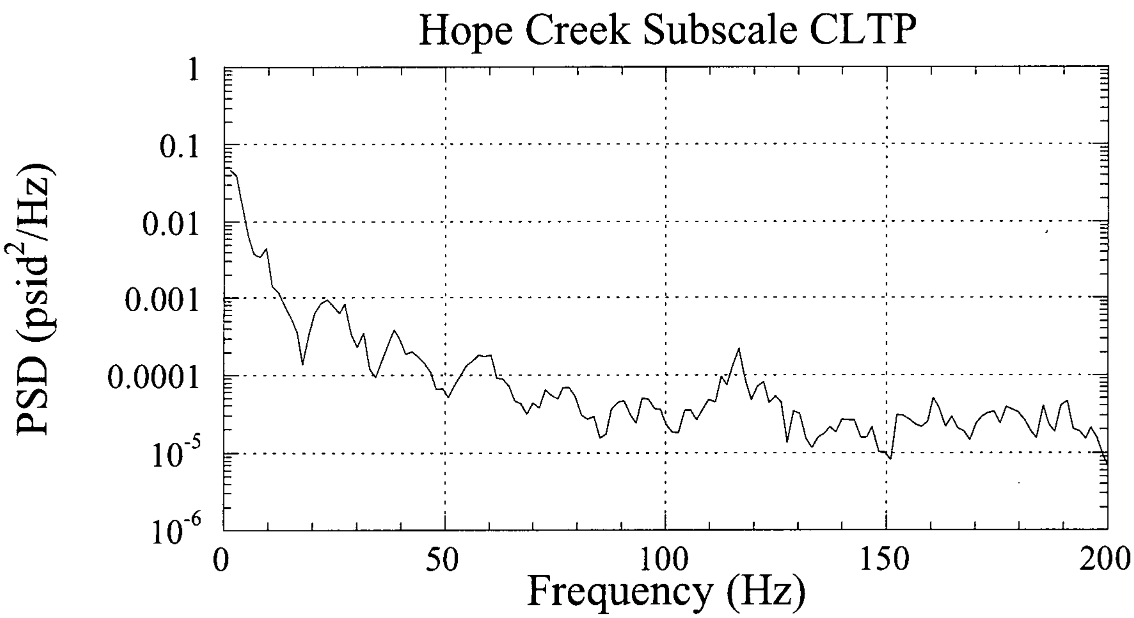

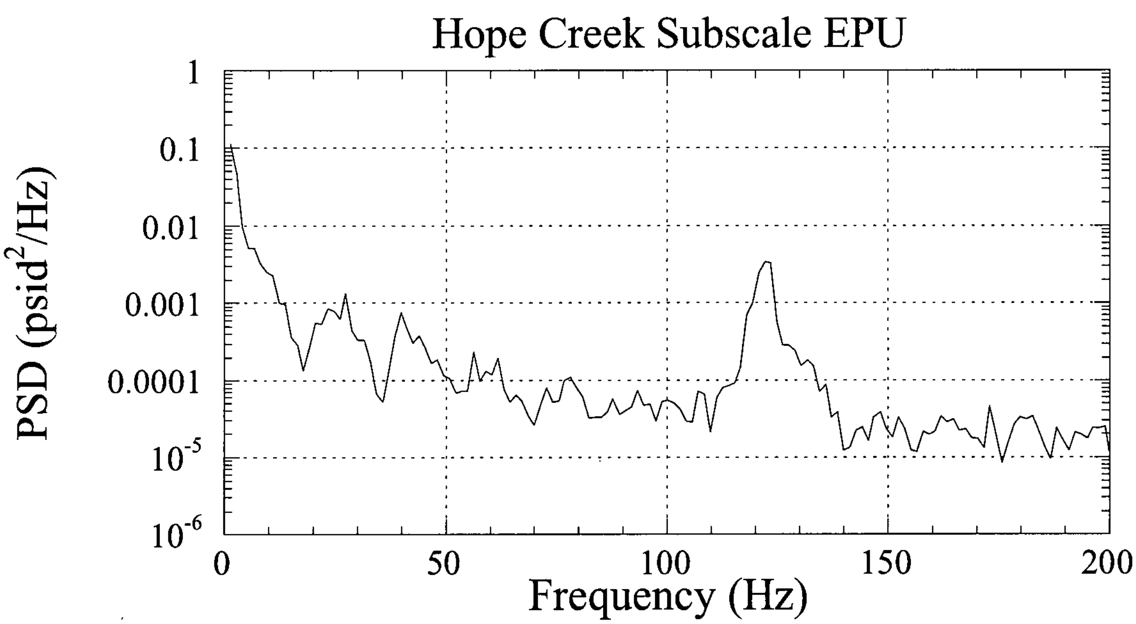

Figure 3.2. PSD comparison of pressure transducer data at CLTP (top) and EPU (bottom) conditions, for main steam line A, downstream location.

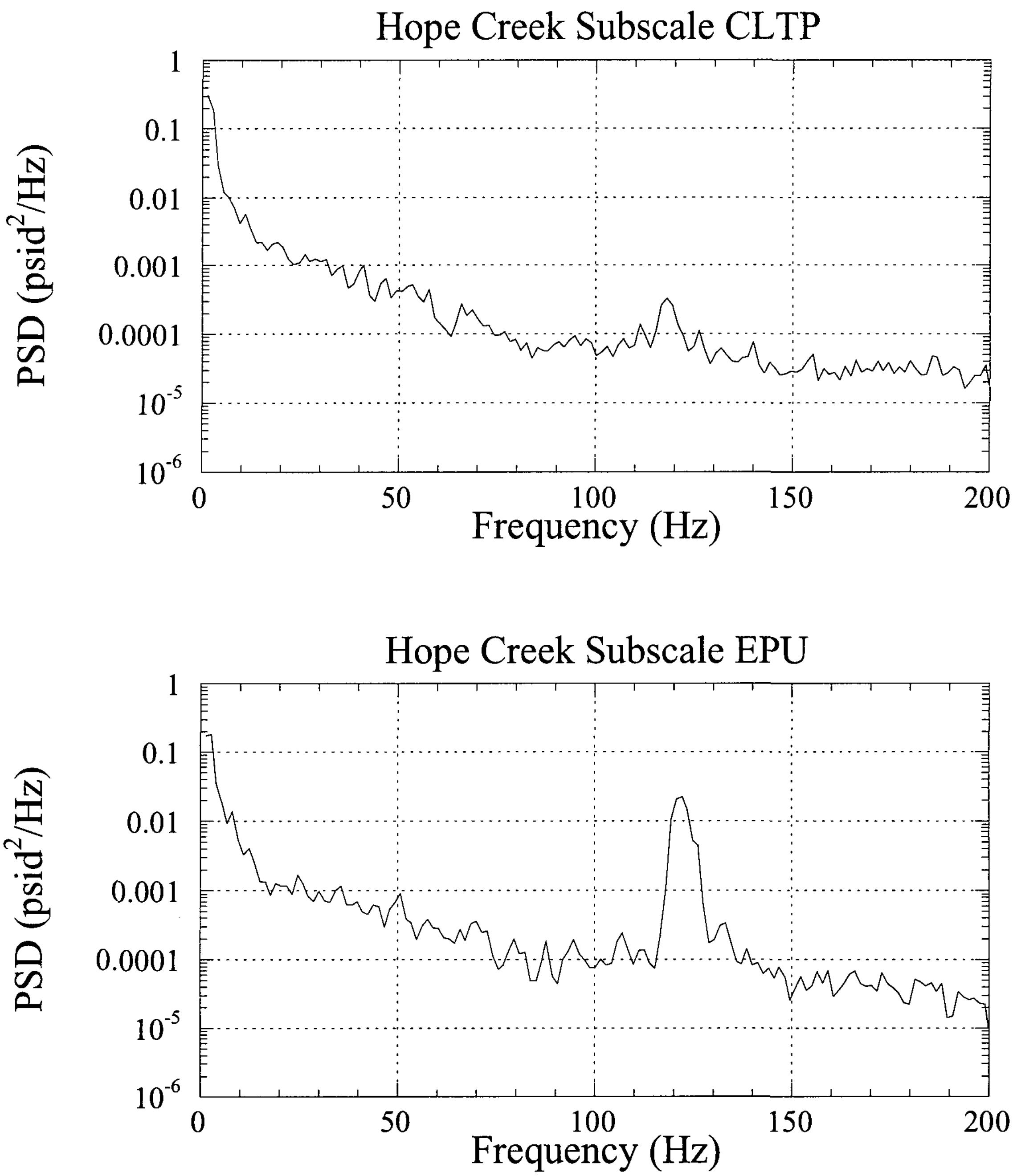

Figure 3.3. PSD comparison of pressure transducer data at CLTP (top) and EPU (bottom) conditions, for main steam line B, upstream location.

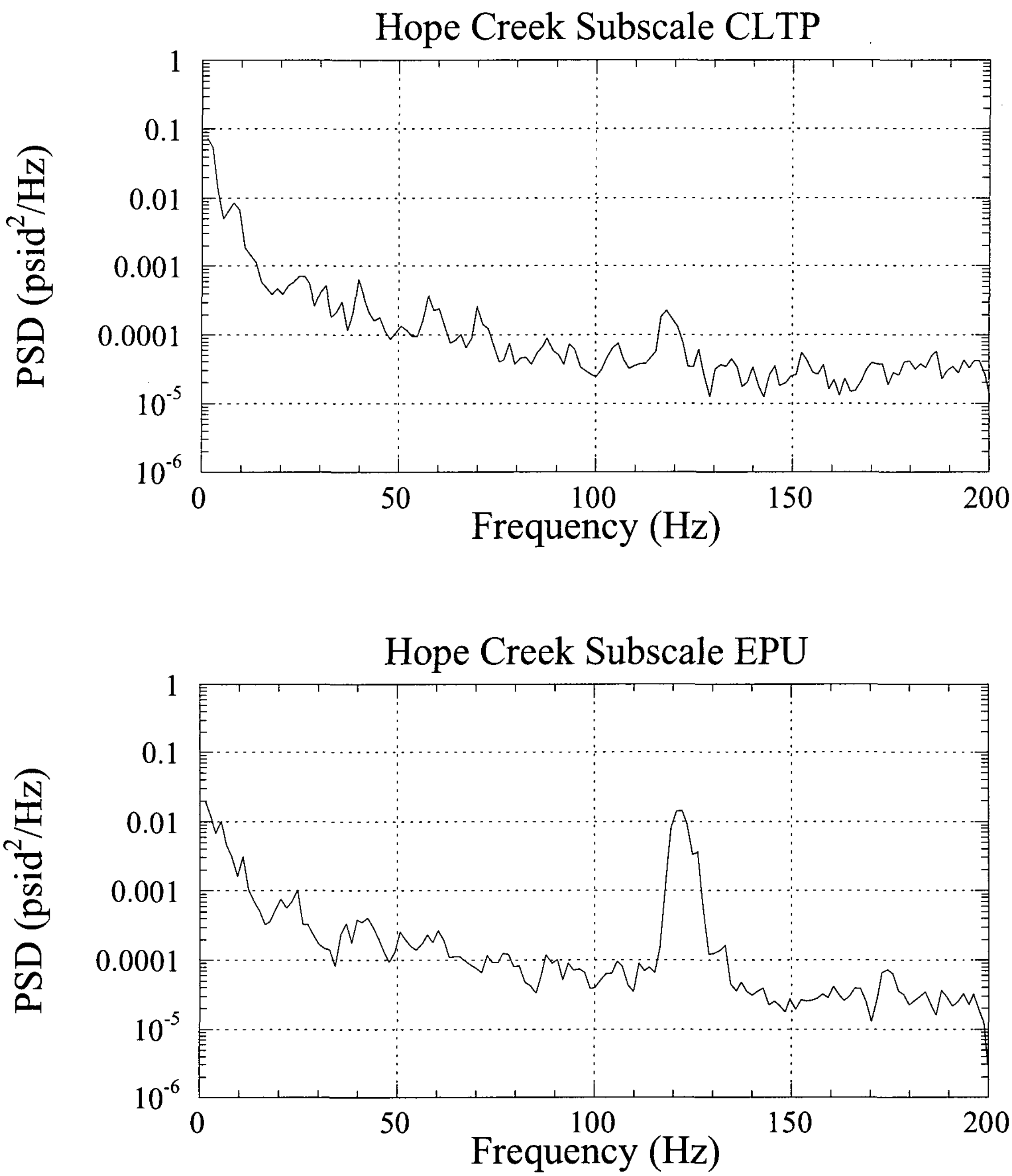

Figure 3.4. PSD comparison of pressure transducer data at CLTP (top) and EPU (bottom) conditions, for main steam line B, downstream location.

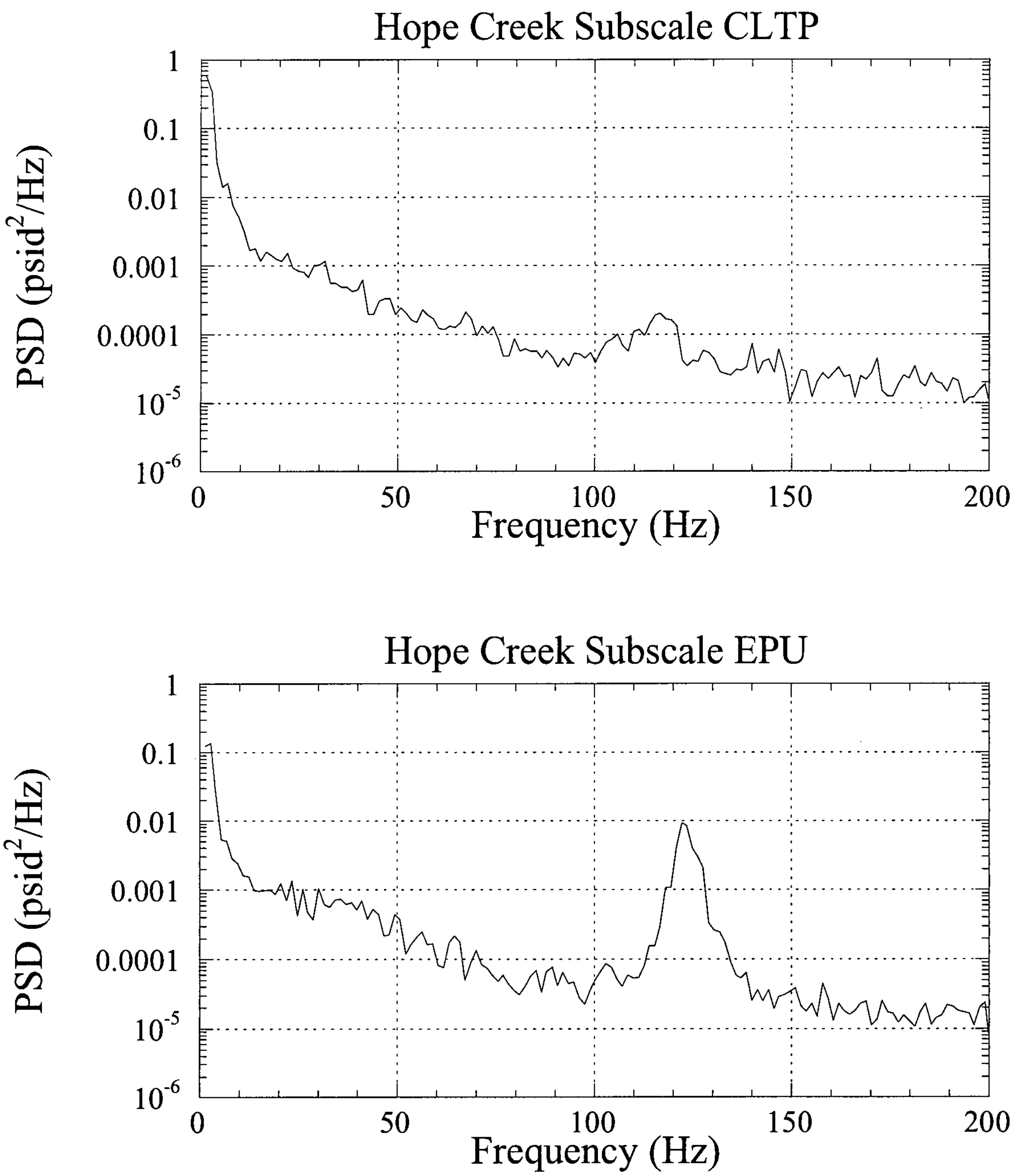

Figure 3.5. PSD comparison of pressure transducer data at CLTP (top) and EPU (bottom) conditions, for main steam line C, upstream location.

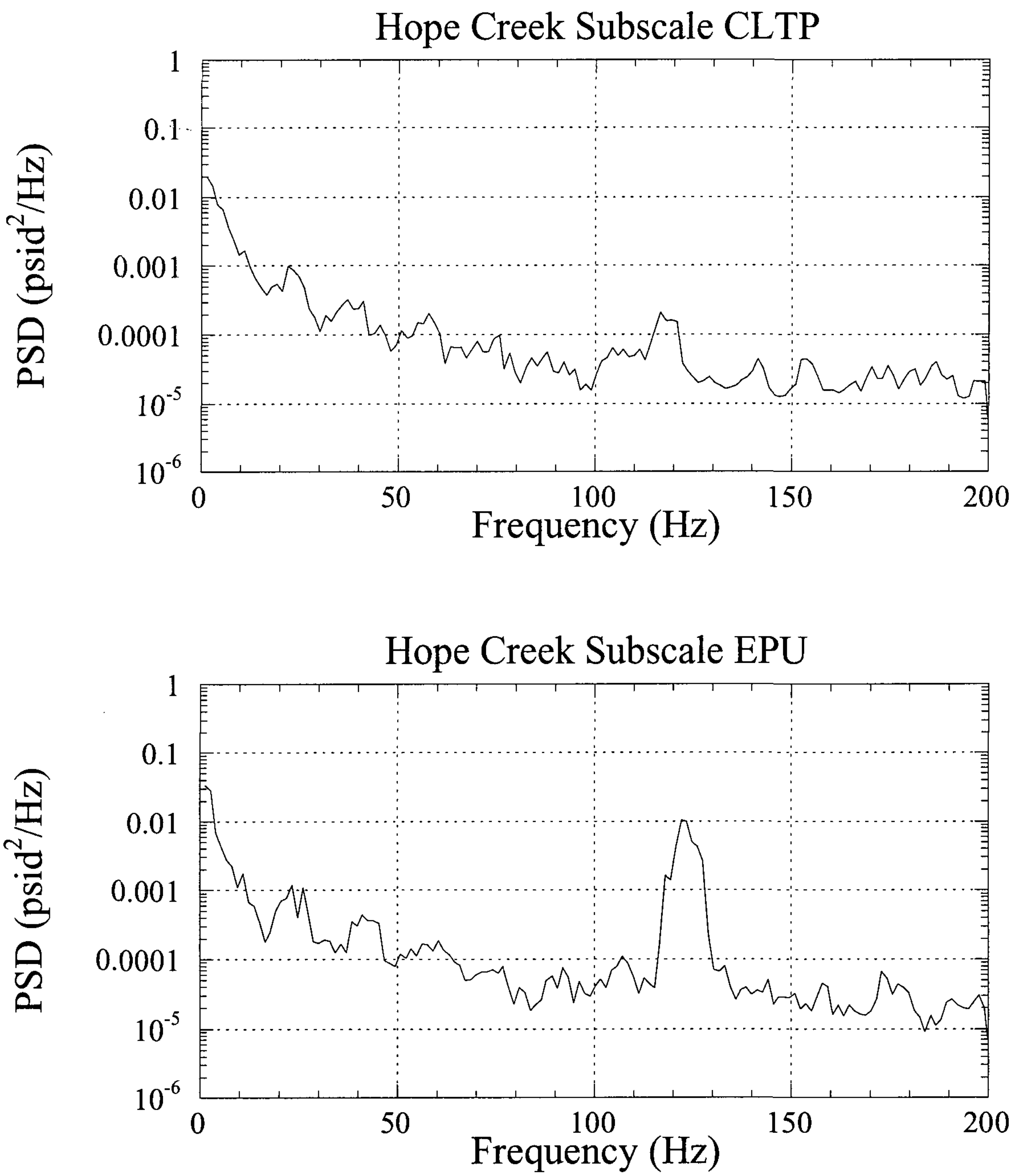

Figure 3.6. PSD comparison of pressure transducer data at CLTP (top) and EPU (bottom) conditions, for main steam line C, downstream location.

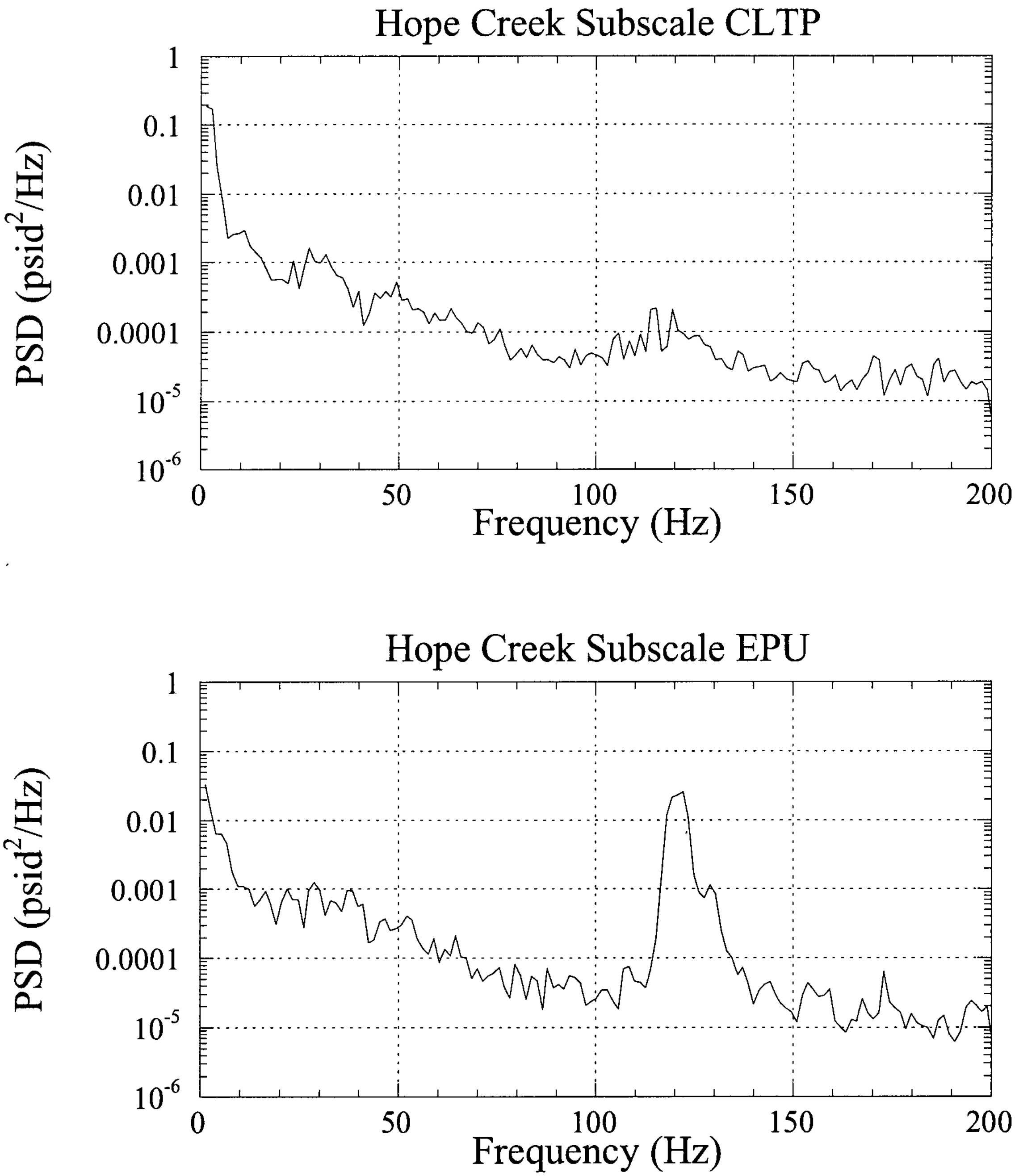

Figure 3.7. PSD comparison of pressure transducer data at CLTP (top) and EPU (bottom) conditions, for main steam line D, upstream location.

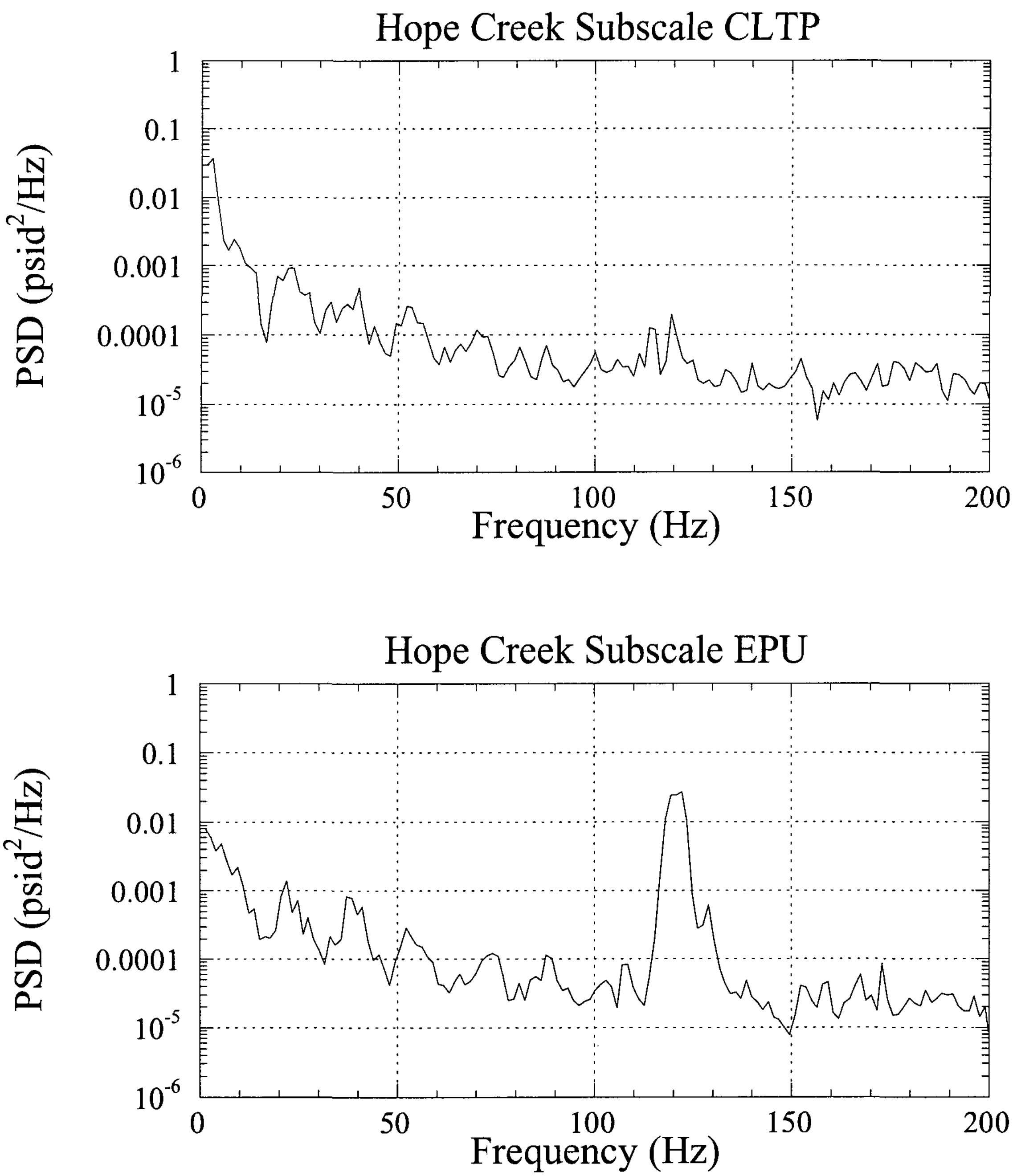

Figure 3.8. PSD comparison of pressure transducer data at CLTP (top) and EPU (bottom) conditions, for main steam line D, downstream location.

Table 3.1. Minimum and maximum pressures, and RMS, in the four main steam lines for the subscale tests at the conditions shown.

CLTP Power Level

Pressure Transducer Location	Minimum Pressure (psid)	Maximum Pressure (psid)	RMS Pressure (psid)
A Upper	-3.50	7.65	1.88
A Lower	-1.91	2.03	0.56
B Upper	-3.01	3.16	1.21
B Lower	-2.23	1.88	0.62
C Upper	-6.21	3.38	1.50
C Lower	-1.12	1.17	0.38
D Upper	-2.96	2.87	0.91
D Lower	-1.32	1.88	0.49

EPU Power Level

Pressure Transducer Location	Minimum Pressure (psid)	Maximum Pressure (psid)	RMS Pressure (psid)
A Upper	-6.45	7.25	2.03
A Lower	-3.47	2.15	0.76
B Upper	-3.94	3.61	1.19
B Lower	-3.73	1.79	0.68
C Upper	-4.09	2.58	1.02
C Lower	-2.08	2.01	0.63
D Upper	-3.13	2.66	0.93
D Lower	-2.05	1.73	0.60

4. Results

The main steam line pressure data were used to drive the verified acoustic circuit model for the HC1 steam dome and main steam lines. Results are presented on a steam dryer low resolution grid by summarizing the peak and RMS pressures expected over the time interval provided in the original data. The low resolution steam dryer grid is shown schematically in Figures 4.1 to 4.4.

4.1 In-Plant CLTP

This information is now provided in [1]. Nodal results are shown in Figure 4.1 of [1] for CLTP conditions for both the original data (derived from data collected in May 2006 on two main steam lines) and the revised data (derived from data collected in February 2007 on four main steam lines). Comparisons were further made at the center edge of the cover plates with the outer bank hoods, on either side of the dryer, at nodes 7 and 99, as shown in Figure 4.3 of [1].

4.2 In-Plant Conservatism

This information is now provided in [1]. Section 4, Figure 4.1, and Figure 4.3 of [1] compare the loading predicted by the February 2007 in-plant data against the loading predicted by the May 2006 in-plant data. This comparison shows that the 2006 data provided conservative results. Figure 4.1 of [1] shows that the maximum differential pressures across the outer band hoods at nodes 7 and 99 are approximately 0.18 psid for the 2006 data and 0.13 psid for the 2007 data. The 2006 data used a conservative algorithm to represent the missing main steam line data.

High resolution loads were subsequently computed, for evaluation by a finite element model (FEM) of the HC1 dryer. The CLTP FEM analysis [5] used the May 2006 in-plant data. As discussed in [1], the February 2007 data demonstrated that the May 2006 data were conservative.

4.3 Subscale CLTP and EPU

4.3.1 SMT Benchmarking to In-Plant Data at CLTP

SMT CLTP information is provided in [1], including a benchmarking of the SMT to the 2007 in-plant data at CLTP conditions. Figure 4.2 of [1] provides the nodal analysis for both the SMT and in-plant data at CLTP conditions. It may be seen from this figure that across all nodes the SMT predicted maximum differential pressures were higher that the in-plant predicted pressures. Comparisons were further made at the center edge of the cover plates with the outer bank hoods, on either side of the dryer, at nodes 7 and 99, as shown in Figure 4.4 of [1].

4.3.2 SMT at CLTP and EPU

Nodal results are shown in Figure 4.5 for CLTP and EPU conditions extracted from the one-eighth scale tests. A non-physical 80 Hz signal has been removed from the in-plant predictions [6]. The peak differential pressure from the subscale EPU conditions, corrected to full scale, is 0.76 psid, compared with a peak differential pressure of 0.17 psid from the corrected subscale CLTP conditions, consistent with the RMS pressure increase recorded in the subscale main steam lines.

Comparisons may be further made at the center edge of the cover plates with the outer bank hoods, on either side of the dryer, at nodes 7 and 99 (as located in Figures 4.1 and 4.3). Pressure time-history and PSD plots are shown in Figures 4.6 and 4.7.

High resolution loads were subsequently computed, for evaluation by a finite element model of the HC1 dryer at EPU conditions. The EPU FEM analysis is found in [7].

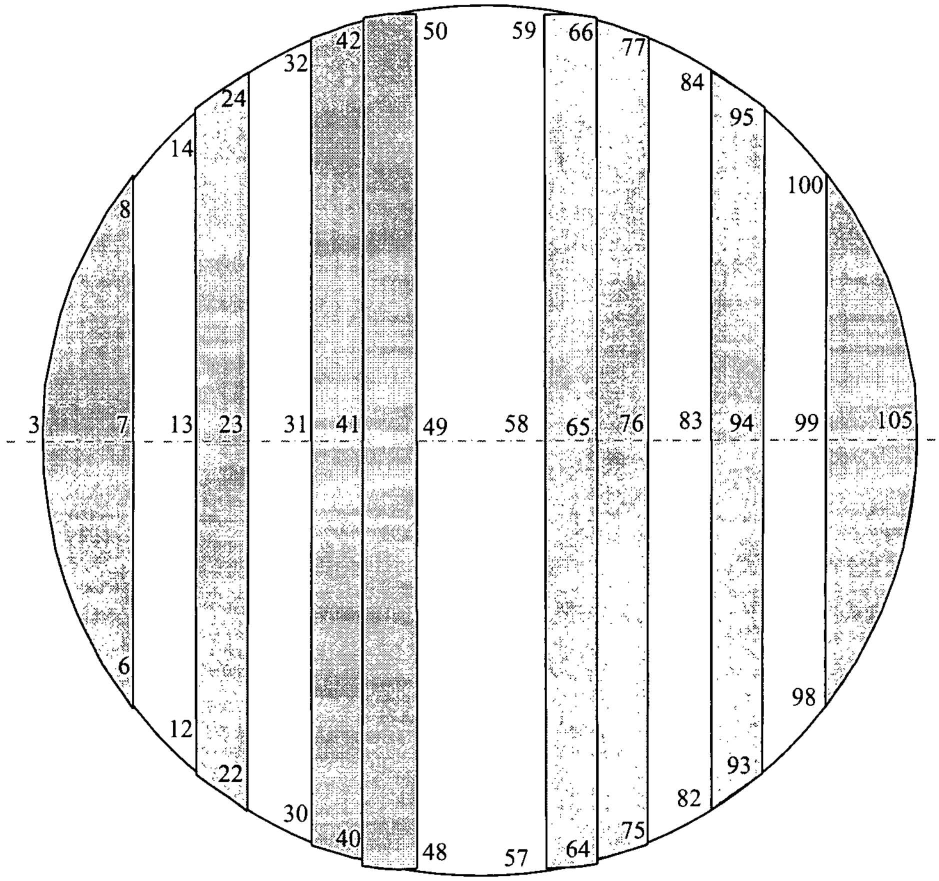

Figure 4.1. Bottom plates pressure node locations, with pressures acting downward in the notation defined here.

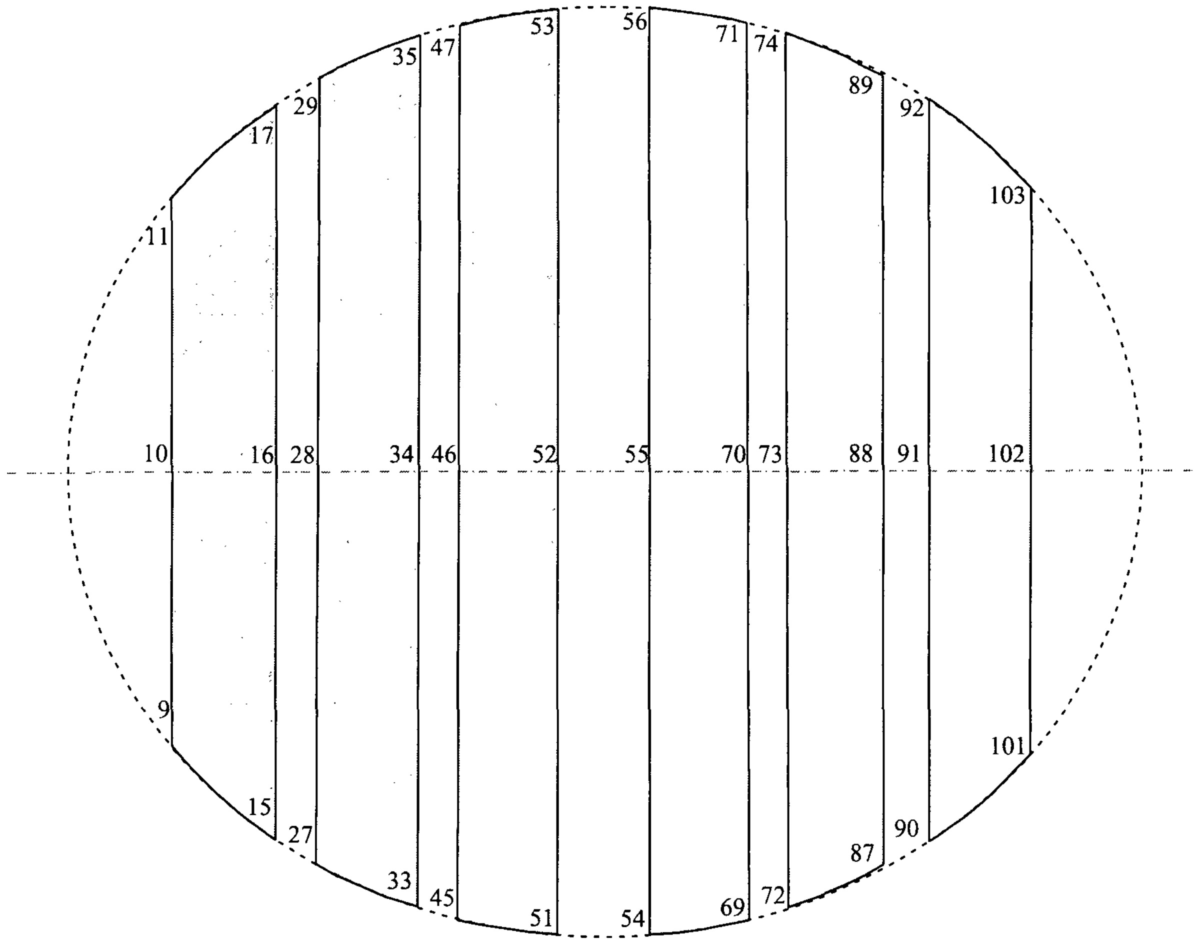

Figure 4.2. Upper plates pressure node locations, with pressures acting downward in the notation defined here.

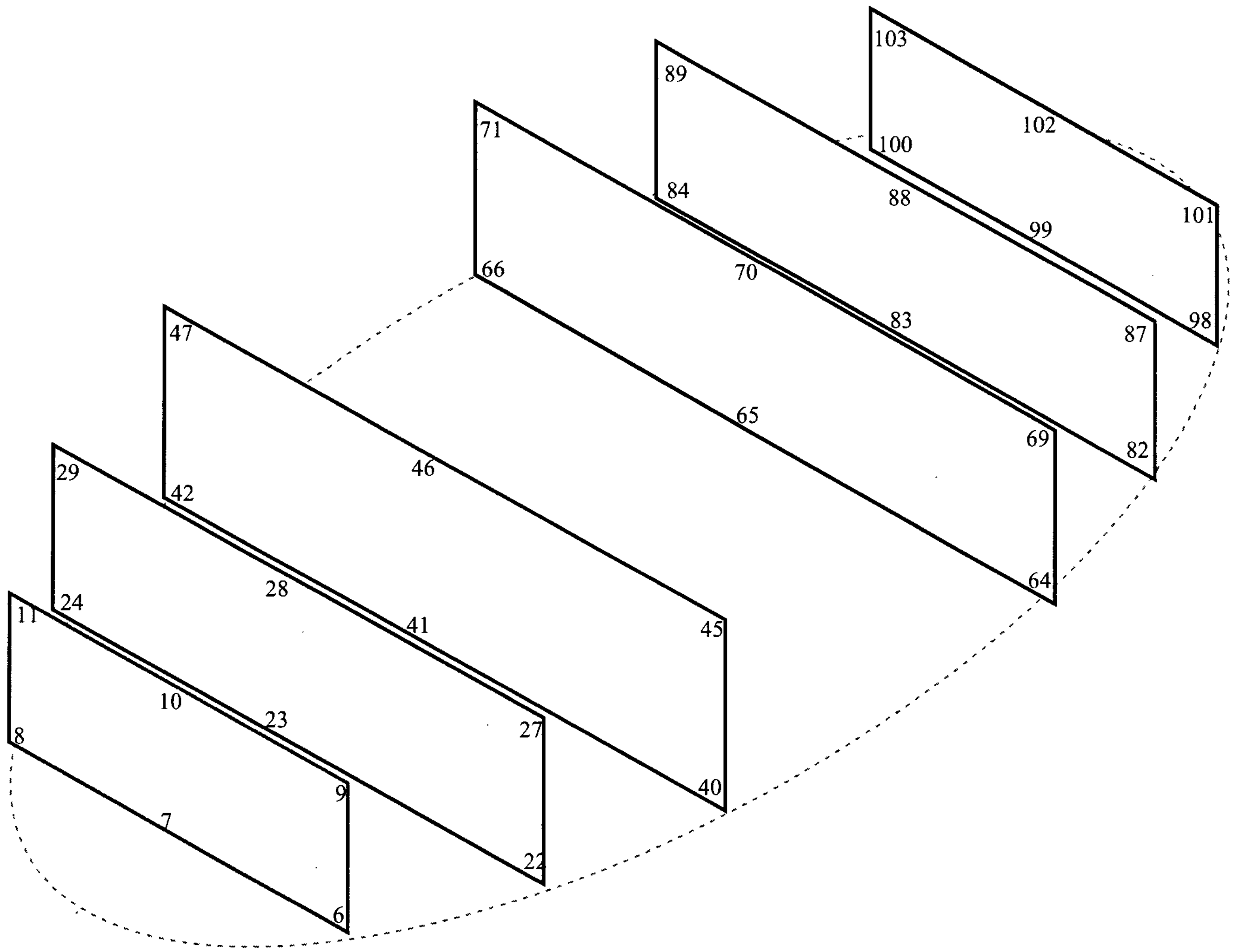

Figure 4.3. Vertical plates: Pressures acting left to right on panels 6-11, 22-29, and 40-47; acting right to left on panels 64-71, 82-89, and 98-103.

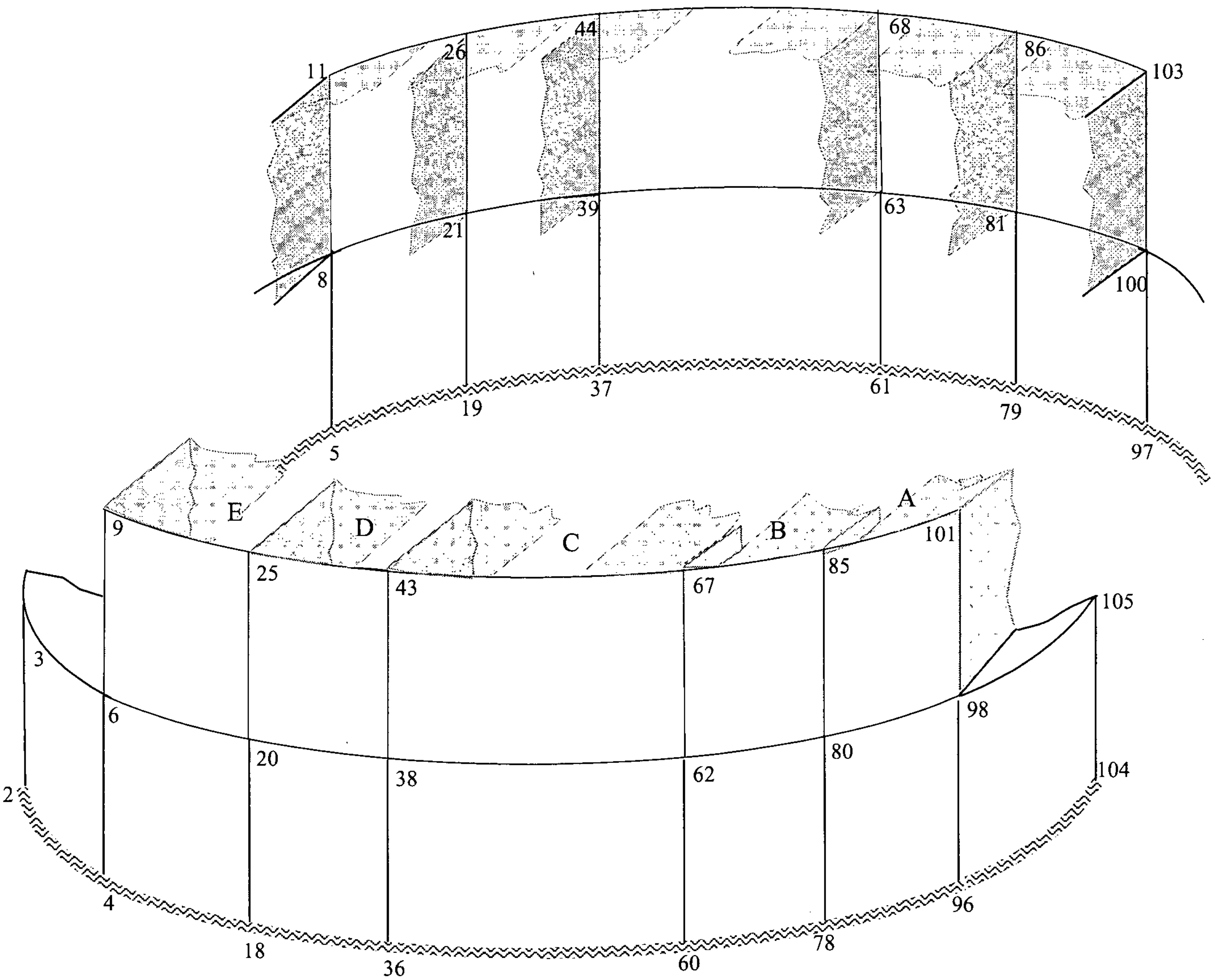

Figure 4.4. Skirt plates: Pressure acting on the outer dryer 0/180 surfaces and the skirt.

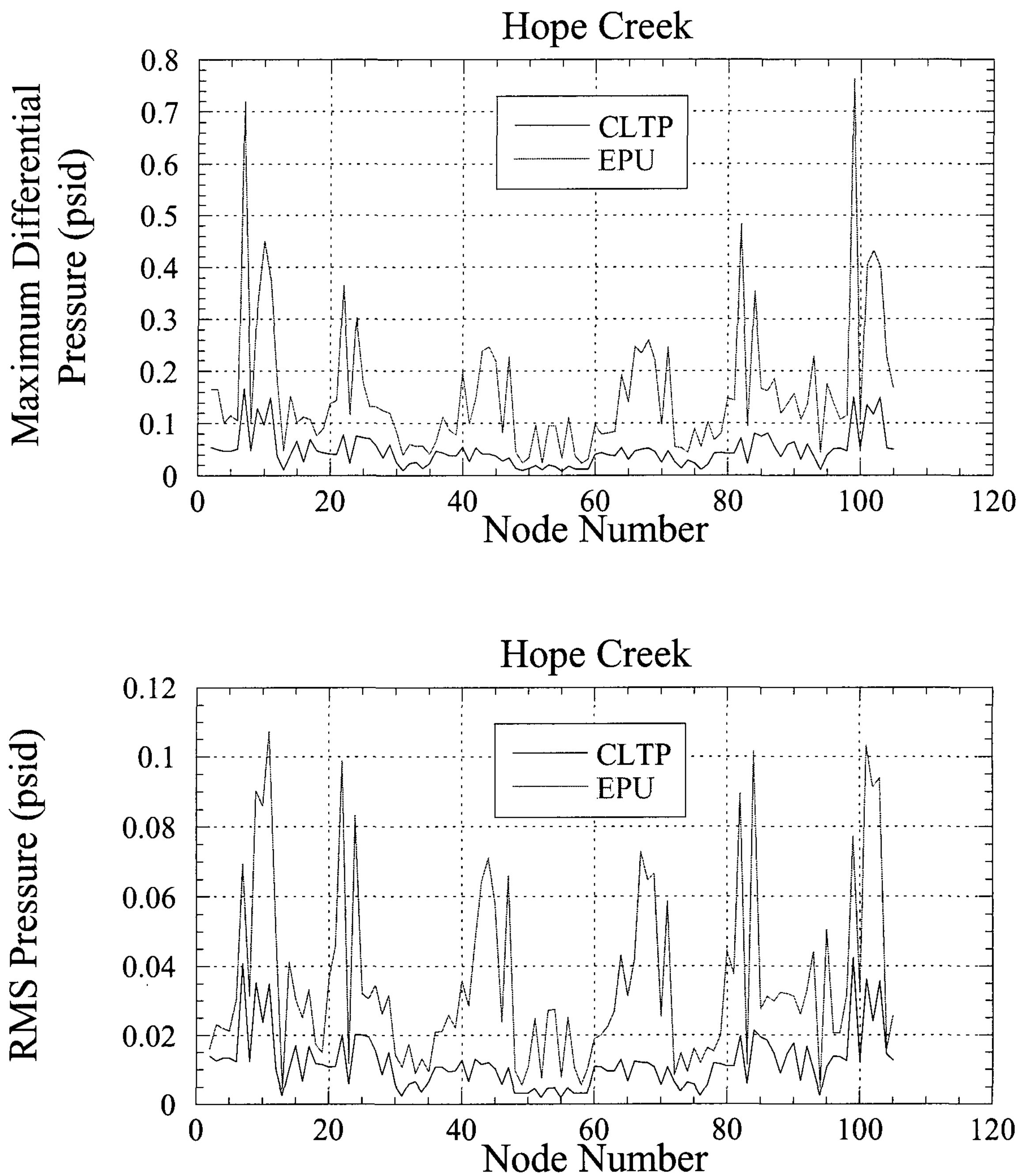

Figure 4.5. Predicted loads at CLTP and EPU power levels as developed by the current methodology to 200 Hz, based on subscale test results. Node 7 is located at the back center edge of the cover plate opposite the C and D main steam lines, while node 99 is located at the back center edge of the cover plate opposite the A and B main steam lines.

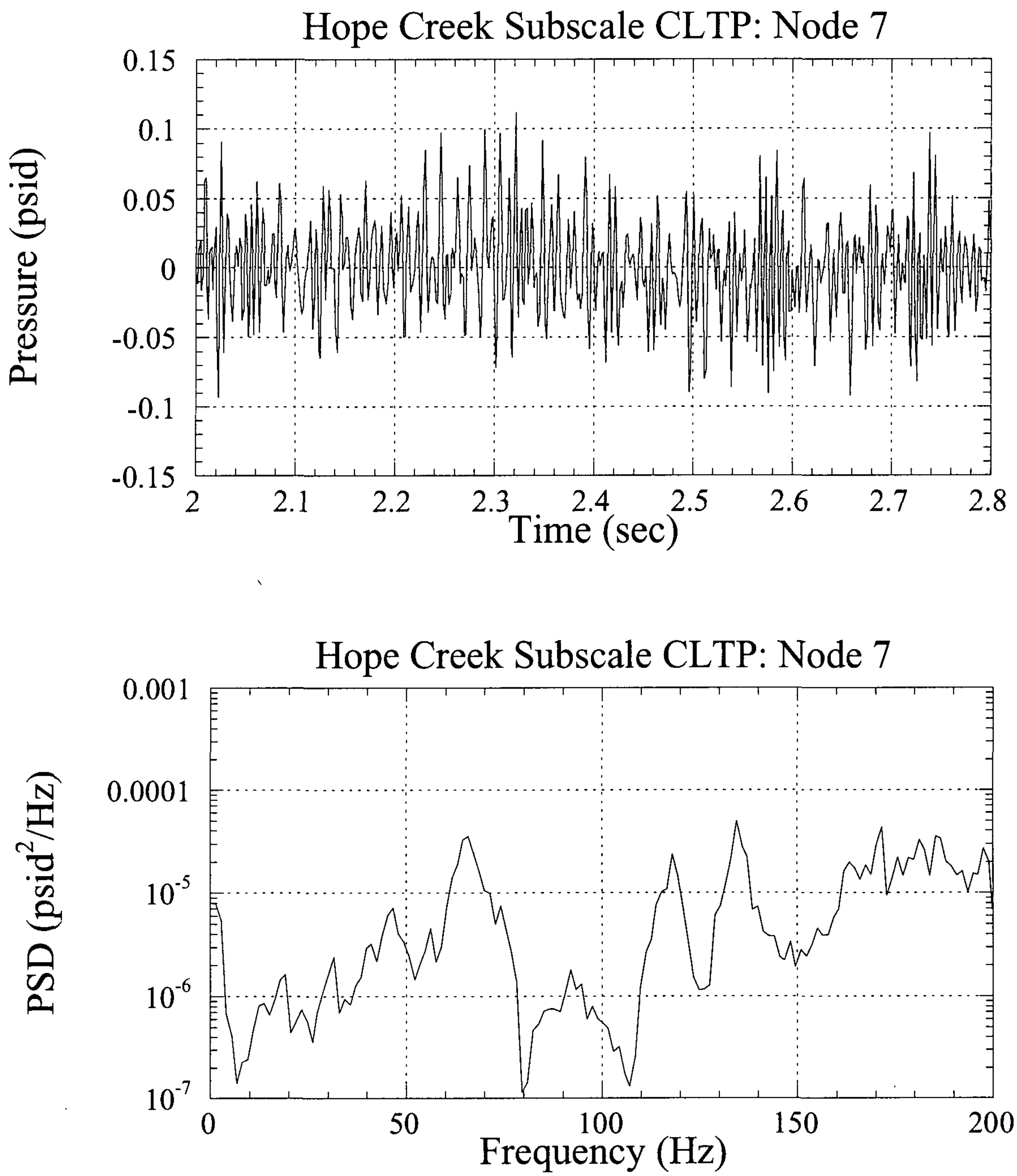

Figure 4.6. Time history and PSD of the predicted CLTP pressure load (extracted from subscale tests) at the center edge of the cover plate with the outer bank hood for node 7 opposite the C-D side of the dryer.

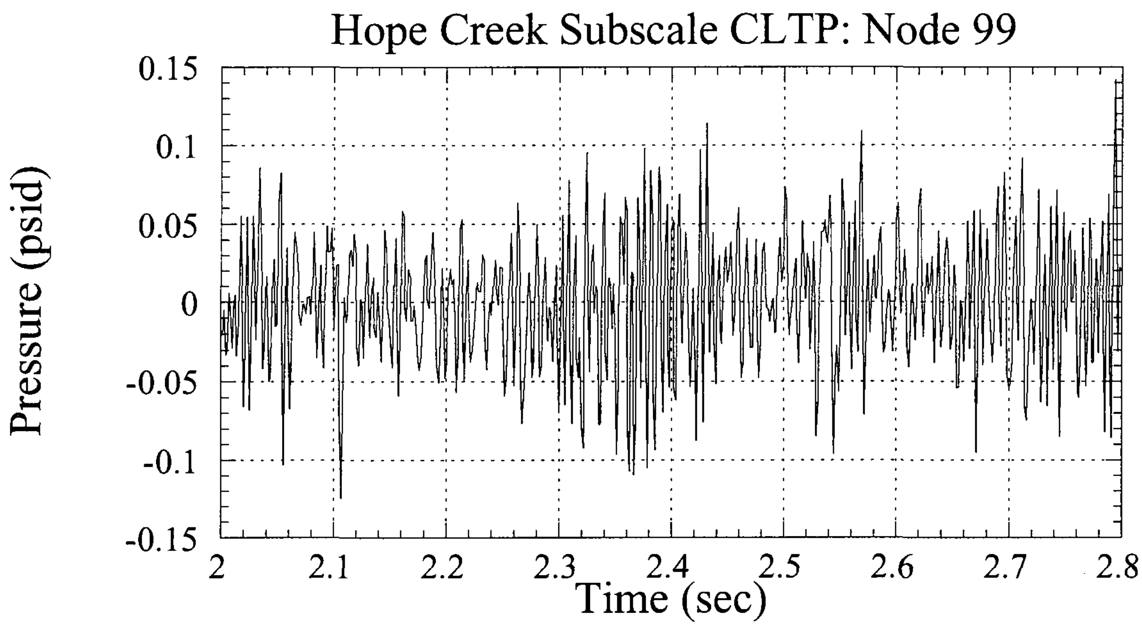

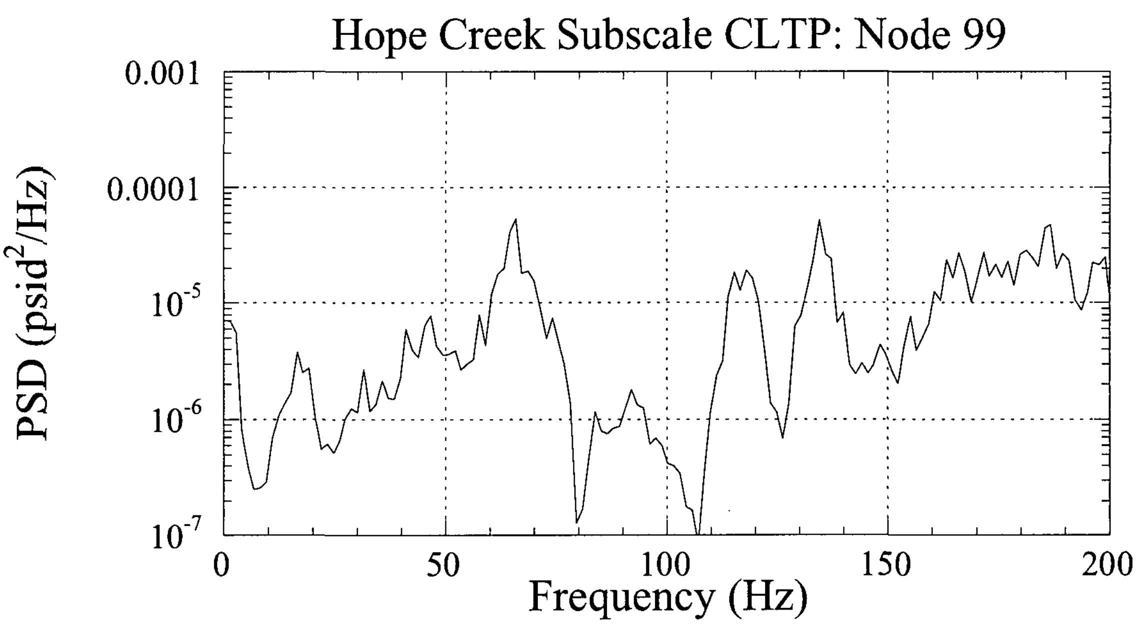

Figure 4.6. (continued) Time history and PSD of the predicted CLTP pressure load (extracted from subscale test results) at the center edge of the cover plate with the outer bank hood for node 99 opposite the A-B side of the dryer.

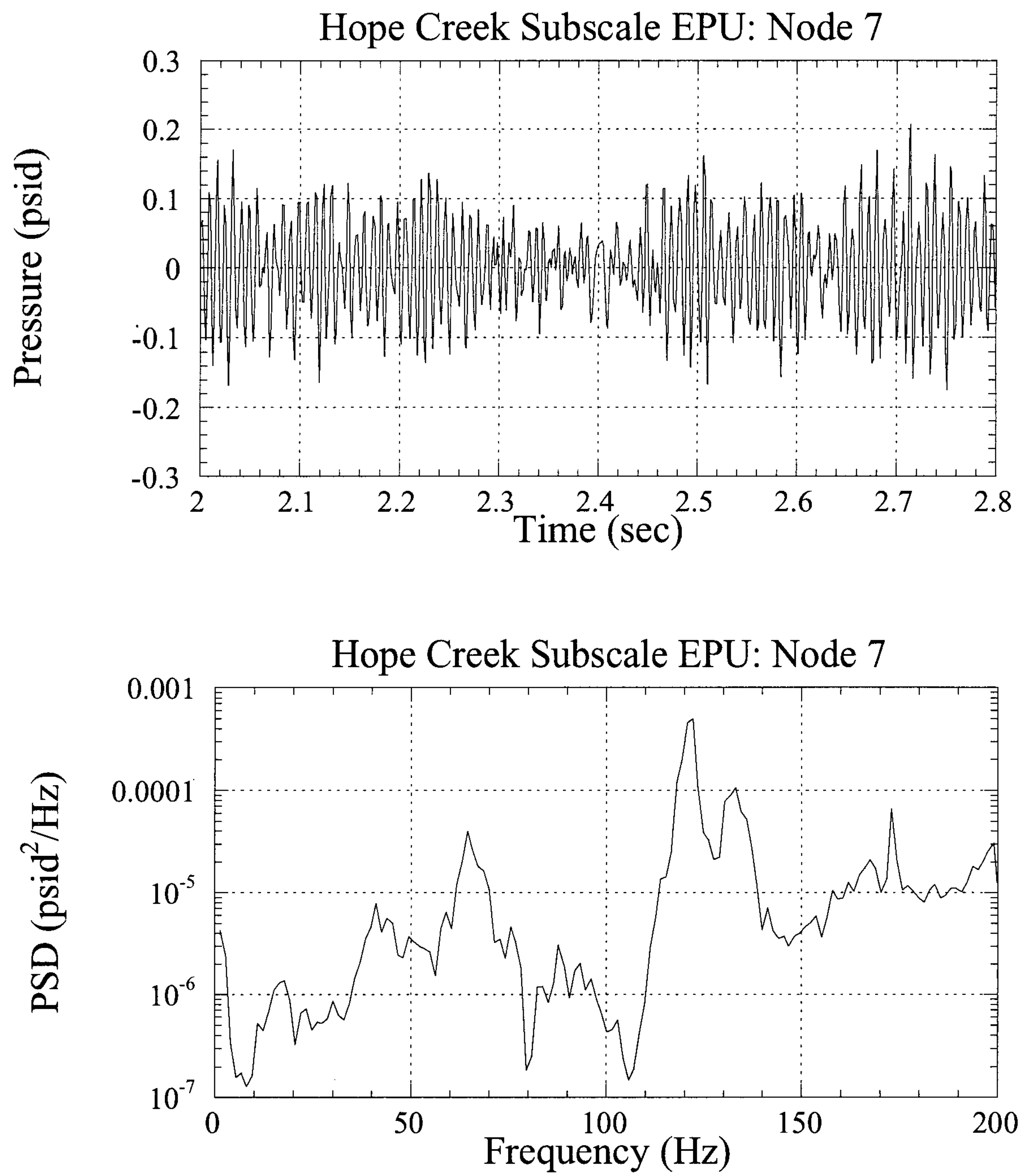

Figure 4.7. Time history and PSD of the predicted EPU pressure load (extracted from subscale tests) at the center edge of the cover plate with the outer bank hood for node 7 opposite the C-D side of the dryer.

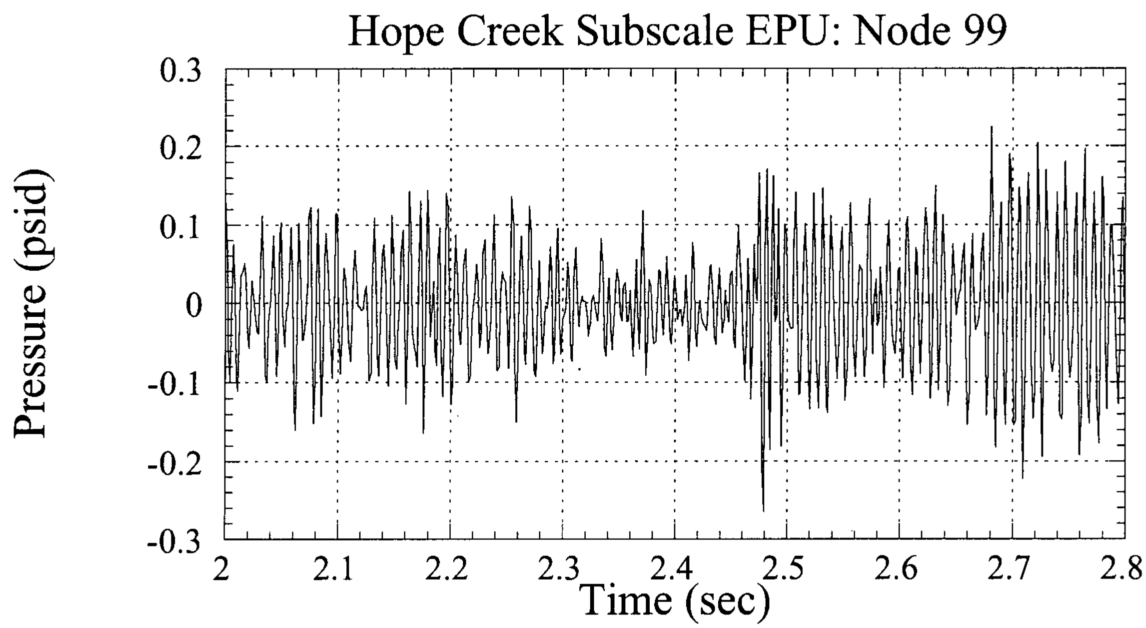

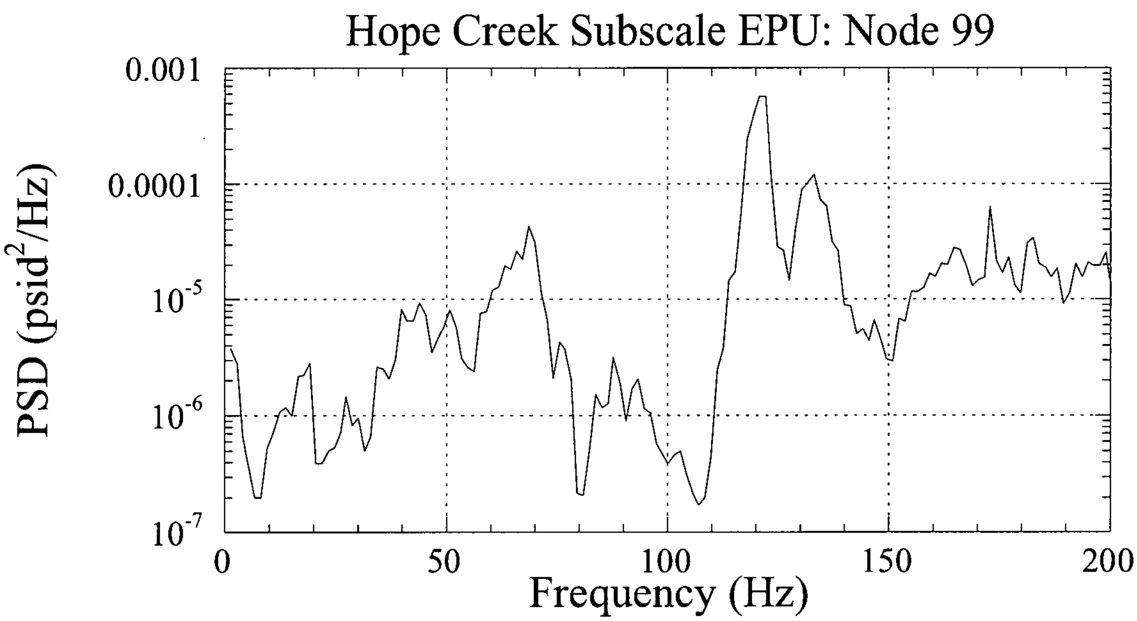

Figure 4.7. (continued) Time history and PSD of the predicted EPU pressure load (extracted from subscale tests) at the center edge of the cover plate with the outer bank hood for node 99 opposite the A-B side of the dryer.

5. Conclusions

Refer to [1] for conclusions on in-plant data and re-benchmarking at CLTP conditions of the SMT to in-plant data.

The C.D.I. acoustic circuit analysis, using one-eighth scale measured data from C.D.I.:

a) Determines that the peak steam dryer differential hydrodynamic loads at EPU power will be less than 0.76 psid.

b) Predicts that the loads on dryer components are largest for components nearest the main steam line inlets and decrease inward into the reactor vessel.

c) Determines that the highest differential pressure load on the dryer occurs at 120 Hz.

6. References

1. Continuum Dynamics, Inc. 2007. Revised Hydrodynamic Loads on Hope Creek Unit 1 Steam Dryer to 200 Hz. C.D.I. Report No. 07-01 (Revision 0).

2. Continuum Dynamics, Inc. 2005. Methodology to Determine Unsteady Pressure Loading on Components in Reactor Steam Domes (Rev. 6). C.D.I. Report No. 04-09 (Proprietary).

3. Continuum Dynamics, Inc. 2006. Bounding Methodology to Predict Full Scale Steam Dryer Loads from In-Plant Measurements (Rev. 1). C.D.I. Report No. 05-28 (Proprietary).

4. Continuum Dynamics, Inc. 2006. Estimating High Frequency Flow Induced Vibration in the Main Steam Lines at Hope Creek Unit 1: A Subscale Four Line Investigation of Standpipe Behavior (Rev. 1). C.D.I. Report No. 06-16.

5. Continuum Dynamics, Inc. 2006. Stress Analysis of the Hope Creek Unit 1 Steam Dryer for CLTP. C.D.I. Report No. 06-24 (Revision 3).

6. Continuum Dynamics, Inc. 2006. High and Low Frequency Steam Dryer Loads by Acoustic Circuit Methodology. C.D.I. Technical Memorandum No. 06-25P.

7. Continuum Dynamics, Inc. 2007. Stress Analysis of the Hope Creek Unit 1 Steam Dryer at EPU Conditions Using One-Eighth Scale Model Pressure Measurement Data. C.D.I. Report No. 06-27 (Revision 2).